NASA Technical Paper 3312

August 1993

Effects of Radiobiological Uncertainty on Vehicle and Habitat Shield Design for Missions to the Moon and Mars

John W. Wilson,
John E. Nealy,
Walter Schimmerling,
Francis A. Cucinotta,
and James S. Wood

NASA Technical Paper 3312

1993

Effects of Radiobiological Uncertainty on Vehicle and Habitat Shield Design for Missions to the Moon and Mars

John W. Wilson
and John E. Nealy
Langley Research Center
Hampton, Virginia

Walter Schimmerling
Universities Space Research Association
Washington, D.C.

Francis A. Cucinotta
Langley Research Center
Hampton, Virginia

James S. Wood
Flight Mechanics and Control, Inc.
Hampton, Virginia

Abstract

Some consequences of uncertainties in radiobiological risk due to galactic cosmic ray (GCR) exposure are analyzed for their effect on engineering designs for the first lunar outpost and a mission to explore Mars. This report presents the plausible effect of biological uncertainties, the design changes necessary to reduce the uncertainties to acceptable levels for a safe mission, and an evaluation of the mission redesign cost. Estimates of the amount of shield mass required to compensate for radiobiological uncertainty are given for a simplified vehicle and habitat. The additional amount of shield mass required to provide a safety factor for uncertainty compensation is calculated from the expected response to GCR exposure. The amount of shield mass greatly increases in the estimated range of biological uncertainty, thus escalating the estimated cost of the mission. The estimates are used as a quantitative example for the cost-effectiveness of research in radiation biophysics and radiation physics.

Introduction

Human exposure to radiation during space exploration is an unavoidable occupational hazard. However, if the probability that crew members will experience deleterious effects can be adequately reduced, this risk may be judged acceptable when mission objectives and other mission risks are considered. The risks are characterized as either stochastic or deterministic. The main stochastic effect is cancer induction. The three main deterministic effects are prodromal response, temporary sterility, and lens opacity. The current criteria for defining acceptable risk in the United States are those recommended by the National Council on Radiation Protection and Measurements (NCRP). The criteria are based on the analysis of annual fatality rates from occupationally related accidents and the need to control early radiation effects, which may adversely impact the ability of the astronaut to perform required tasks safely. On this basis, risk of stochastic effects has been defined in terms of the increase in lifetime probability, above the natural incidence, that the radiation exposure will result in fatal cancer. According to this criterion, an acceptable risk level limits the excess fatal cancer probability to 3 percent or less (ref. 1). Such a risk was considered acceptable for routine space operations in low Earth orbit (LEO). Similarly, dose limits are given in reference 1 that limit deterministic effects to ensure mission safety and astronaut health.

In LEO, the predominant exposure is from electrons and protons. For this radiation, extrapolations based on existing radiobiological data may be adequate, and quantities commonly used in radiation protection, such as the dose D, the dose equivalent H, and quality factor Q, relating D to H as follows:

$$H = QD \tag{1}$$

have been used to establish radiation limits (see table I). In equation (1), the quality factor is a function of the linear energy transfer (LET) of the radiation. The exact functional form of the quality factor is prescribed in the process of setting radiation guidelines, making Q a legislated quantity rather than the result of a measurement. However, the dependence of Q on LET, $Q(L)$, is intended to reflect a judgment related to the dependence of relative biological effectiveness (RBE) on LET at the anticipated levels of exposure. For a radiation field with a distribution of LET values, the use of an average quality factor is required (ref. 1). The average quality factor is determined as follows:

$$\overline{Q} = \frac{1}{D} \int Q(L) \frac{dD}{dL} dL \tag{2}$$

where dD/dL is the dose contribution per unit LET interval.

Table I. Exposure Limits for LEO Operations

Exposure time	Exposure limits, Sv, for—		
	Blood-forming organs	Eye	Skin
30 days	0.25	1	1.5
Annual	0.5	2	3
Career	[a][2 + 0.075 (Age − T_o)]	4	6

[a]Average career dose-equivalent limit for both male (T_o = 30) and female (T_o = 38) astronauts for a 3-percent increase of cancer risk (ref. 1).

For galactic cosmic rays (GCR) and, in particular, for the highly charged energetic (HZE) nuclei that constitute the biologically most significant component of GCR, these equations may no longer provide an adequate description of the radiation risk (ref. 1). Evidence that the description of the risk is inadequate has been provided by the measurement of sister chromatid exchanges in resting human lymphocytes irradiated with ^{238}Pu α-particles (ref. 2), by the observation of abnormalities in stem cell colonies surviving similar α-particle irradiation (ref. 3), and by the partial disintegration of chromosomes after irradiation with high-energy heavy ion beams to simulate space radiation (ref. 4). In these examples, a quality factor related to RBE becomes meaningless because at doses comparable to that delivered by one particle (or a few particles) and for radiation effects that are not manifest for low-LET radiation (e.g., X rays), the RBE becomes infinite. Thus, new methods to predict the risk resulting from exposure to GCR radiation must be developed.

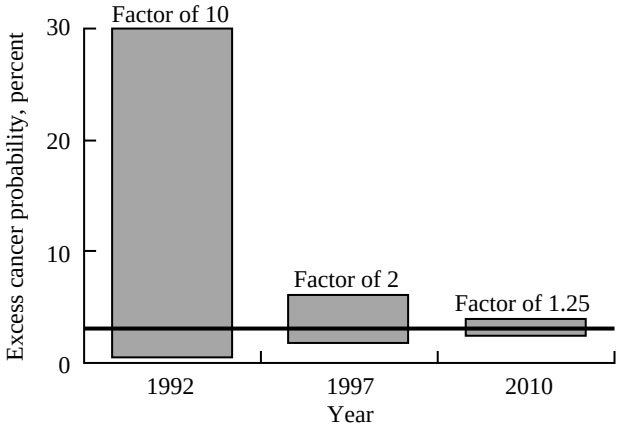

Figure 1. NASA Space Radiation Program estimates for current and projected risk uncertainties.

In addition to the problems posed by radiation effects not observable at reference doses of low-LET radiation, estimates of risk are uncertain, even for known radiation effects. In the United States, the NASA Space Radiation Health Program has been established to sponsor research intended to further "the scientific basis for the radiation protection of humans engaged in the exploration of space" (ref. 5). A main objective of the program is to reduce the uncertainty in the prediction of radiation risk so that it is within a factor of 2 (50- to 200-percent range) by 1997 and within a factor of 1.25 ($\pm$25 percent) by 2010 as shown in figure 1. The present uncertainty in risk predictions is estimated to be as large as an order of magnitude (10- to 1000-percent range). This is no more than an educated guess, obtained with the assumption that the uncertainty of a factor of 10 is the uncertainty in the prediction of shielding effectiveness (a factor of 2 to 3) and the uncertainty in predicting biological response to HZE particles (a factor of 4 to 5).

Engineers and mission planners must compensate for these uncertainties to ensure that risk limits are not exceeded. Depending on policies and engineering judgment, the compensation required may be one, two, or more standard deviations (with a Gaussian distribution assumed for the uncertainties). For example, if predictions of risk are considered accurate only within an order of magnitude (factor of 10), the shielding of a spacecraft required to remain below a 3-percent excess cancer risk may in reality be designed for a 30-percent excess cancer risk; this risk is clearly not acceptable. The shield mass would have to be greatly increased to ensure that the excess cancer risks did not exceed 3 percent in view of such large uncertainties.

The compensation required for uncertainty can significantly increase costs. If the shielding thickness of a lunar or martian habitat has to be increased by a factor of two, the total shield volume (mass) increases by more than a factor of two. As the volume increases, the time necessary to assemble the habitat increases for a constant work force; increasing the work force requires transporting more mass to orbit per launch or increasing the number of launches. The increased assembly time would increase extravehicular activity (EVA), and the Shuttle cannot presently support extensive EVA. Time is also quantized; the duration of one mission is expected to be 30 to 60 days. If the habitat assembly extends beyond the duration of one mission, the number of launches doubles. If habitat assembly extends beyond two missions, the number of launches triples. Faster assembly of the habitat requires more machinery; the cost of machinery development, testing, and deployment must then be added to the cost of launching the machinery mass. These relationships are depicted in figure 2.

Another example of the complex effect of increases in shielding to account for uncertainties in risk prediction may be seen in figure 3, a schematic view of a typical solar energetic particle (SEP) event. The X rays arrive at the lunar surface within 9 min of the start of the event and can be used as a warning signal to crews. Significant particle fluxes begin to be experienced Δt_1 minutes (or hours) later and would rapidly increase until, at a time Δt_2 after the initial warning, the radiation levels inside a shielded rover vehicle on the lunar surface would exceed

allowed limits. Before this time, the crew must find a storm shelter or return to the safety of the shielded base.

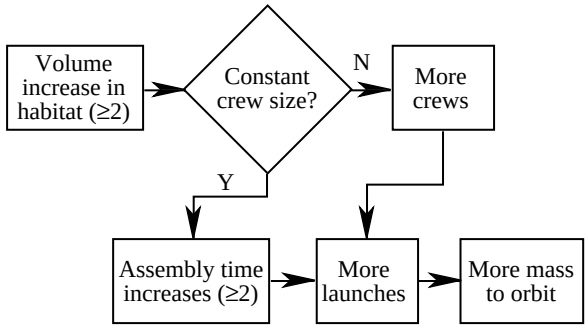

Figure 2. Logic diagram showing effects of increased shielding on launch requirements.

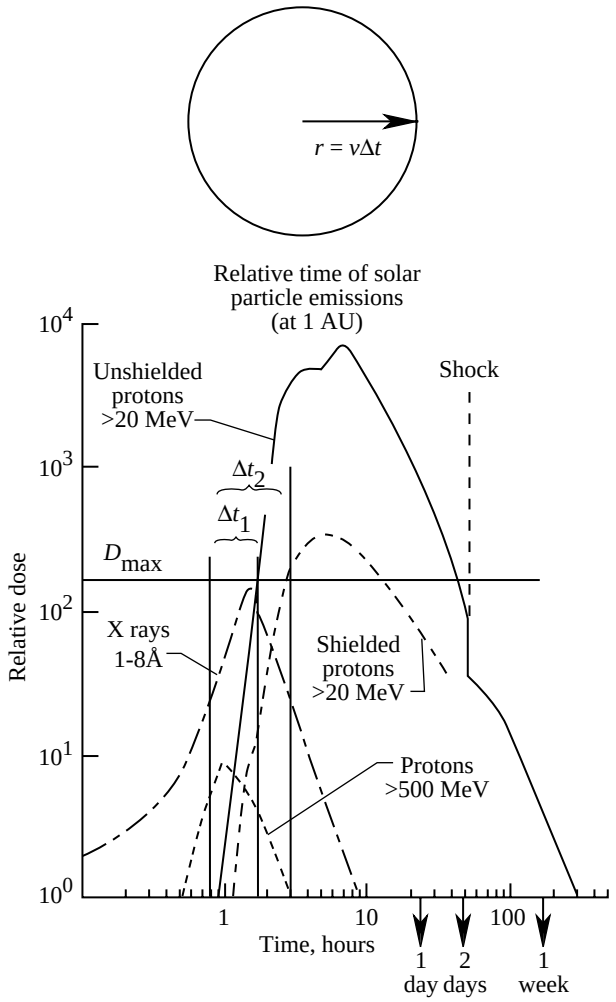

Figure 3. Limits on exploration range due to possible SEP events. Area = $\pi v^2(\Delta t)^2$; v depends on shielding and determines fuel requirements; Δt depends on shielding and forecasting ability.

The maximum distance that a lunar rover vehicle can be allowed to travel away from a safe location is given by $v\Delta t$, where v is the velocity of the rover. This distance gives the maximum area that can be explored in one sortie, $A_{\max} = \pi v^2(\Delta t)^2$. Thus, at constant velocity, the sortie range is determined by the warning time and by the rover speed. Higher rover speed may require more fuel, more batteries, or larger engines and may also result in less vehicle reliability. Hence, more spare parts or more backup vehicles may be required. All these requirements necessitate mass lifted from Earth. Increasing rover shielding to extend sortie time may reduce the speed of the rover and result in similar increased mass requirements. Establishing shielded refuges to increase the surface range requires an increase in construction time and may lead to supply mission restrictions that are quantized (more launches). Another alternative is to delay surface exploration until a permanently inhabited base is established.

Current estimates of GCR radiation exposure (ref. 6) clearly show that the radiation risk limits the design and operation of lunar and martian missions. The risk uncertainties discussed previously will have a large impact on mission design. Trade-offs between uncertain biological risk, design costs, and the investment in research required to reduce these uncertainties heavily favor the research investment. As beneficial as research is for missions of long duration, what are the effects of uncertainties in biological response and shielding properties on missions of shorter duration? This question will be considered in the following sections.

There is interest within NASA to plan a return to the Moon for a mission with a duration of 45 to 60 days to establish the first lunar outpost (FLO).[1] Unlike a mission to Mars or a permanent lunar base, where exposure to HZE particles plays a dominant role, the total GCR dose for a 60-day mission is 70 mSv or less (ref. 6). The current main shield was designed for protection from a possible SEP event and not primarily for protection from HZE exposure. In the following sections, a simple shielding configuration is assumed and its modification to account for the uncertainties in risk prediction is calculated to illustrate the preceding considerations. The low incidence of GCR exposure allows for linear approximations using risk coefficients. The model is used to estimate the effects of biological risk uncertainty on shield mass and projected mission costs. Following the 60-day lunar mission, the analysis is applied to

[1]NASA Exploration Program Office Report: *FLO Mission Overview*, May 1992.

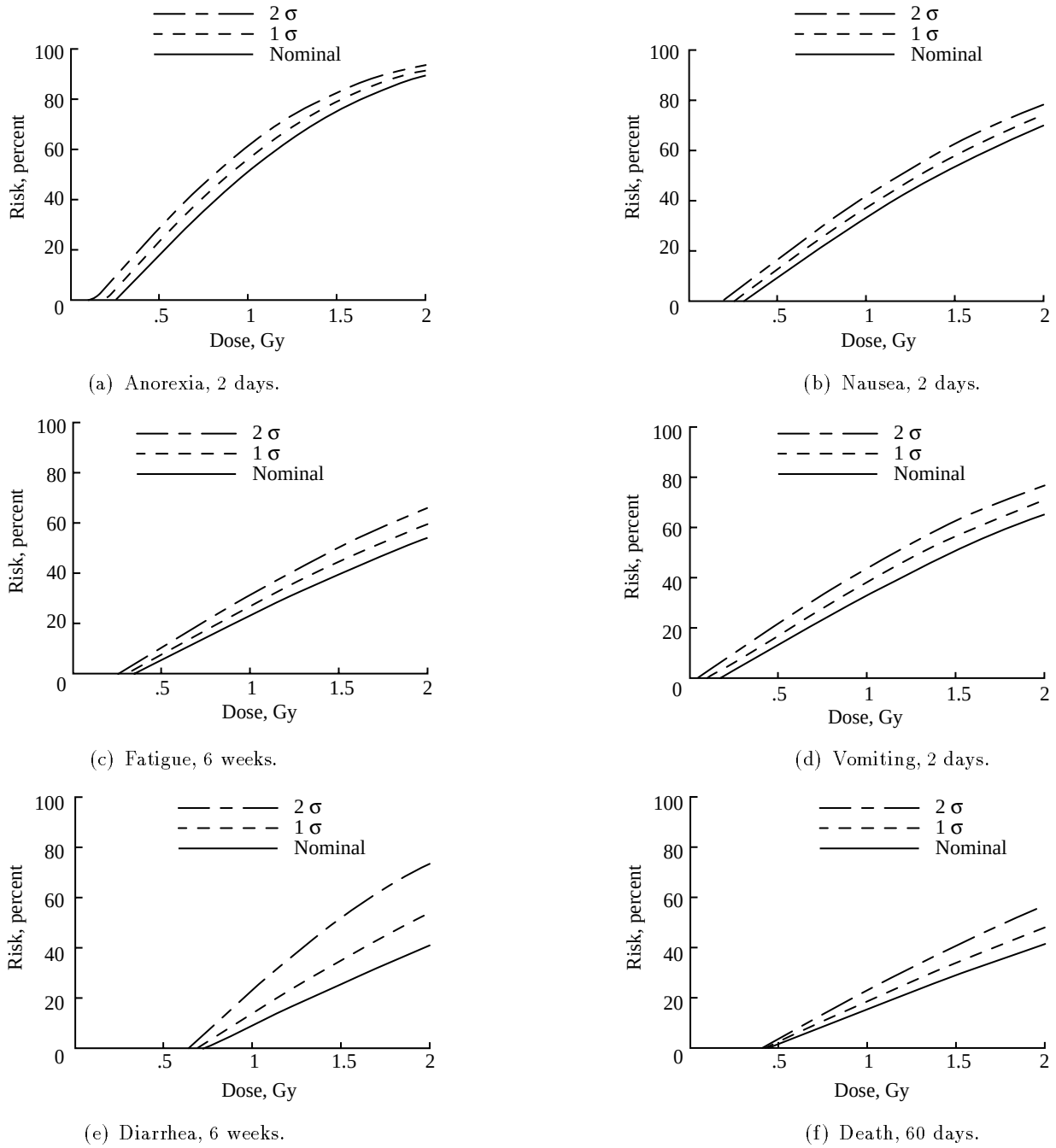

(a) Anorexia, 2 days.

(b) Nausea, 2 days.

(c) Fatigue, 6 weeks.

(d) Vomiting, 2 days.

(e) Diarrhea, 6 weeks.

(f) Death, 60 days.

Figure 4. Risk of prodromal response within specified postexposure time period because of X ray exposure.

a 6-month lunar mission and two missions to explore Mars.

While the methodology is quite general and can be applied to other space exploration missions, it is essential to incorporate the effects of uncertainty in radiation risk estimates into engineering designs at the earliest possible stage, so that a realistic assessment of the impact of radiation protection limits on mission costs and launch mass can be established. The purpose of the present report is to explore the plausible effect of the radiobiological risk uncertainties, the change in mission design to reduce the risks to acceptable levels, and an evaluation of the redesign cost to perform a safe mission. The approach described herein is also intended to offer some insight into the problems of extrapolating data from the current LEO radiation limits and applying this data to lunar and martian missions.

Radiation Risk Data Base

Deterministic radiation effects are identified by relating the severity of injury to the degree of exposure. Even though a given level of exposure will result in different levels of injury among a group of individuals, the severity of injury for a given individual increases with increased exposure level. Deterministic effects are associated with the sensitive parenchyma cell populations, their associated less mature populations, and their support systems. The injury in most tissues results mainly from the inability of the cells to undergo division (clonogenic death), which is the functional purpose of the stem populations (ref. 7). The primary tissues involved are bone marrow, skin, ocular lens, and intestinal lining. Early response risk functions derived by the Space Science Board of the National Academy of Sciences for low-LET radiation (ref. 8) are shown in figure 4. These data were mainly derived from radiation therapy patients with high naturally occurring rates of symptoms. As a consequence, the radiation-induced responses had large corrections. Later evaluations of data presented in reference 1 from victims accidently exposed to radiation were used to correct the vomiting response curves. The 1σ bounds are used here for risk evaluations.

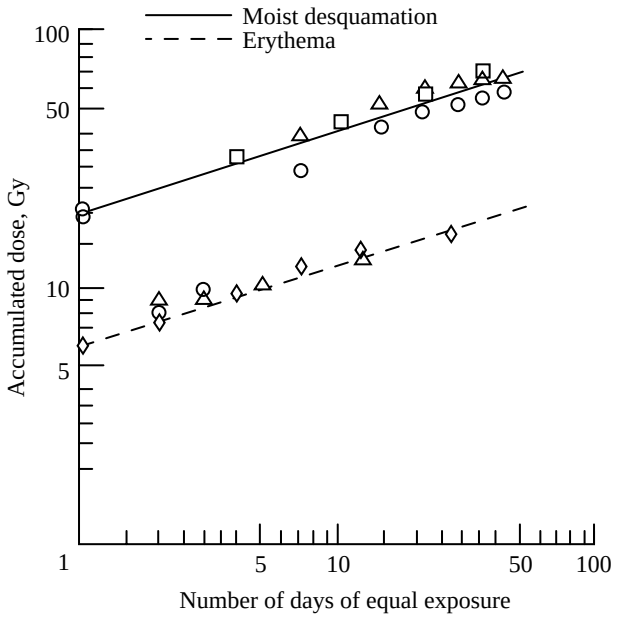

Figure 5. Dose protraction effects on median response to skin exposures for low-LET radiations (ref. 9).

Repair of radiation injury occurs on the cellular level and on the tissue system level. Rate of repair is readily revealed at a given exposure level by fractionated exposure schedules. These schedules are determined by dividing the amount of exposure into equal levels that are portioned over a time period. The dose level at which 50 percent of a human population shows early skin response to X rays for various fractionated schedules is shown in figure 5. It is seen from the figure that 20 percent of the damage is repaired over a 3-day fractionated schedule.

Stochastic radiation effects are identified by the probability of occurrence, not severity, being related to degree of exposure. Although a given level of exposure will represent some level of risk for a given group, the risk within a given subgroup may be higher or lower at the same exposure level. The risks of the subgroup are related to factors such as age, sex, genetic disposition, and environmental influences (ref. 9). The occurrence of cancer, a prime stochastic effect, is associated with changes in the genetic structure of a cell, for which the normal controls against cell division have been inactivated. Obviously, cells that have suffered clonogenic death do not contribute to stochastic effects.

The repair of radiation injury to the genetic material of a cell (transformation) occurs at the cellular level. The promotion of a transformed cell to a cancer cell occurs when the cell division process starts; this promotion is tissue dependent (ref. 7). Cell repair processes could be studied using fractionated exposure schedules, but only a small amount of data on humans is available for making risk estimates. In the analysis of data on humans, the relative risk model is usually favored. For this model the age-specific cancer risk is written (ref. 9) as

$$\gamma(D_\gamma) = \gamma_o\left[1 + f(D_\gamma)\ g(\beta)\right] \tag{3}$$

where γ_o is the naturally occurring rate; $f(D_\gamma)$ is the dose response, usually assumed to be linear-quadratic in D_γ; and $g(\beta)$ depends on age, sex, age at exposure, and environmental factors. If risk of subsequent exposures is additive, the quadratic dose term vanishes as the number of fractions becomes large. The quadratic term is known from studies of the nuclear weapons used in World War II. We assume γ_o and $g(\beta)$ for lifetime risk for exposure at age 35. The excess risk of fatal cancer is then

$$\begin{aligned} R(D_\gamma) &= \gamma(D_\gamma) - \gamma_o \\ &= 0.03 D_\gamma \left(1 + \frac{D_\gamma}{1.16}\right) \end{aligned} \tag{4}$$

where D_γ is the dose equivalent in sieverts. The nonlinear term is negligible for highly protracted exposures. Equation (4) rests mainly on γ-ray exposures, although a small neutron contribution was present, mainly in the Hiroshima event (ref. 9).

High-LET Exposure Risks

The dose used for low-LET radiation to characterize the human response data in the previous section is best understood by considering how the dose is deposited in individual cells. The energy absorbed within a cell is ε_i, and the total dose within the tissue cell population is given as

$$D = \frac{\Sigma\varepsilon_i}{VN_E} = \frac{\Sigma\varepsilon_i}{VN_H}\frac{N_H}{N_E} \tag{5}$$

where N_E is the total number of cells exposed, V is the cell volume, and N_H is the total number of cells "hit" during exposure. At a low dose, not all cells are hit, so the number of hit cells N_H is less than the number of cells exposed. Only as $N_H \to N_E$ does the value of D have meaning in terms of tissue response (ref. 10). The fraction of cells hit at low exposure ($N_H \ll N_E$) is

$$\frac{N_H}{N_E} \approx \sigma_g\,\phi \tag{6}$$

where σ_g is the geometric cross section and ϕ is the particle fluence. The cross section can be larger than the geometric cross section because of the δ-ray diffusion, but equation (6) is assumed here to be a first-order approximation. The particle fluence ϕ is related to the absorbed dose and LET as $\phi = (6.24D)/L$ (for ϕ in particles/μm^2, D in Gy, and L in keV/μm). For γ-rays, L_γ corresponds to 0.2 keV/μm, and the corresponding ϕ_γ is an effective γ-ray fluence that is dependent on the photoabsorption coefficient and the actual fluence. The event spectra are approximated by a continuous distribution $f(\varepsilon)\,d\varepsilon$, so the dose is written as follows:

$$D = 6.24\sigma_g\frac{D}{L}\frac{\Sigma\varepsilon_i}{VN_H} \equiv 6.24\frac{\sigma_g D}{VL}\int \varepsilon f(\varepsilon)d\varepsilon \tag{7}$$

Equation (7) shows that $0.16(VL/\sigma_g)$ is the average event size in keV within the cell. This relationship is related to microdosimetric relations, where the average lineal energy (energy of event divided by cell mean chord) is numerically equal to the LET for the usual triangular event distribution (ref. 11). The fraction of cells hit and the mean event energy are shown for a 1-Gy exposure in figure 6. The fraction of hit cells in the multihit region is according to Poisson statistics. The low-LET region ($L < 5$ keV/μm) involves exposure of a large fraction of the cells, while very few cells are directly irradiated at high-LET ($L \gg 5$ keV/μm) when hit cells receive large energy deposition (>100 keV). On this basis, we expect the biological response to a 1-Gy exposure by radiations of greatly different LET to be substantially dissimilar. Yet, the important factors in predicting tissue response depend on the probability of cell injury at a given event level, the efficiency of cellular repair, and the role of the cell in the function of the tissue. As an example, we have calculated the geometric hit frequency, the initial level of cell injury, and the unrepaired cell injury that lead to clonogenic death (ref. 12) in C3H10T½ mouse cells. Figure 7 shows that the cell is most often hit by hydrogen and helium ions, but with small probability of injury. The figure also shows that the repair efficiency is high, which leaves little permanent injury. Conversely, the silicon and iron ions have high probabilities of injury when hits occur and near zero efficiencies of repair. As a consequence, most clonogenic death from GCR exposure is because of ions with LET above 10 keV/μm, such as ions heavier than carbon, and these exposed cells show minimal repair. As a result, dose protraction for GCR exposure is less effective in reducing the biological response.

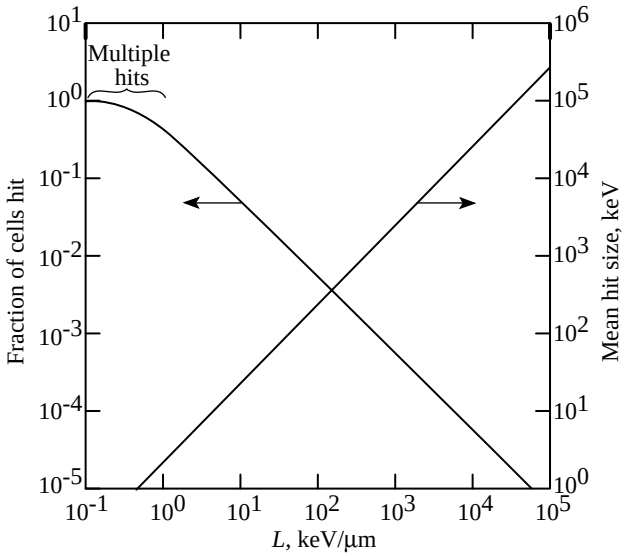

Figure 6. Nonuniformity of exposure at the 1-Gy level for a typical tissue system. $D = 1$ Gy; $\sigma_g \approx 100$ μm^2.

The conventional method of extrapolating the data base for human exposure to high-LET radiation is expressed in equation (1). Equation (1) follows from an analogy with the RBE given for γ-ray and ion exposure levels D_γ and D_i, which result in the same biological end point by the equation

$$\text{RBE} = \frac{D_\gamma}{D_i} \tag{8}$$

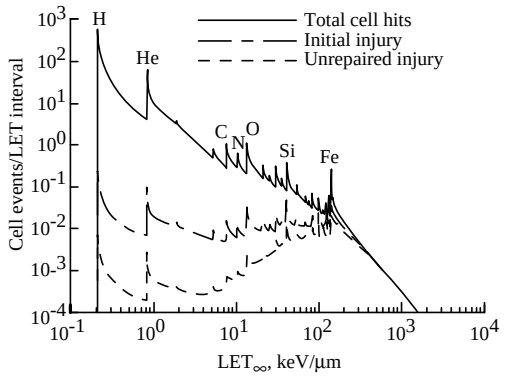

Figure 7. Survival response in stationary C3H10T½ cells for a 1-year GCR exposure.

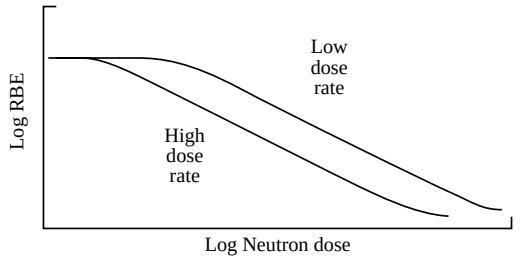

Figure 8. Schematic of RBE for neutron exposure at different dose rates.

Table II. RBE_M for Fission Neutron Exposures

[From ref. 11]

Biological end points	RBE_M
Tumor induction	≈3–≈200
Life shortening	15–45
Transformation	35–70
Cytogenic studies	40–50
Genetic end points in mammalian systems	10–45
Other end points:	
Lens opacification	25–200
Micronucleus assay	6–60
Testes weight loss	5–20

As noted, the quality factor is a defined quantity (not given by a measurement) and represents trends of measured RBE in cell culture, plant, and animal experiments. The RBE values depend on end point, dose, dose rate, and quality of the radiation, which is usually represented by LET. It is usually assumed that the RBE reaches a maximum value (RBE_M) at a sufficiently low dose relative to the initial slopes of the response curves of each radiation type (ref. 1). Furthermore, the dose at which RBE_M is achieved is assumed to be dose-rate dependent as shown schematically in figure 8. The values of RBE from which Q is defined as a function of LET are largely for high dose rates at the 0.1-Gy level of exposure. At this level, fission neutrons with $\overline{Q} = 25$ correspond to a γ-ray exposure of 2.5 Gy (i.e., RBE = 25 for these exposures). The RBE_M values for lower levels of exposure and/or lower dose rates are much larger (ref. 11) as shown in table II and occur for lower exposure and dose rates than were used in deriving Q. Since RBE_M is achieved faster at low dose rates, the RBE values in table II may in fact be more appropriate for space exposures. This is one source of the uncertainties in space radiation exposures.

A second source of the uncertainties concerns the response to HZE exposures, for which little is known. It is postulated that there are possible single-ion track effects for which γ-ray exposures have no analog. One such mechanism was suggested by Todd (ref. 13) in which cells exposed at 0.25 Gy outside the track core have a high probability of being transformed, while the dead cells in the track core must be replaced, causing promotion to a cancer growth by this single exposure event (fig. 9). The RBE's for such effects are undefined (infinite), and extrapolation from the present human data base is not possible.

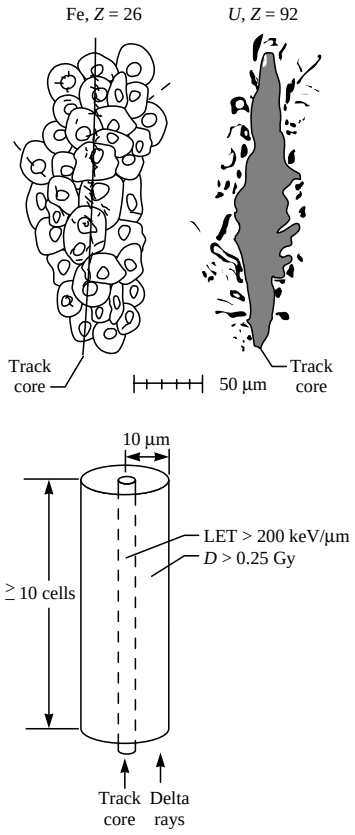

Figure 9. Single-particle effect proposed by Todd in reference 13.

The use of an LET-dependent quality factor as related to dose equivalent implies additivity of diverse components to estimate risk. Such assumptions may underestimate the actual risk, as was discussed by Scott (ref. 14). Furthermore, risks associated with different time intervals are not additive. For low-LET exposures, substantial repair often occurs and results in reduced risk. For high-LET exposures, there are possible dose-rate enhancement effects (ref. 15) in which risk is substantially increased at lower dose rates. (See fig. 10.)

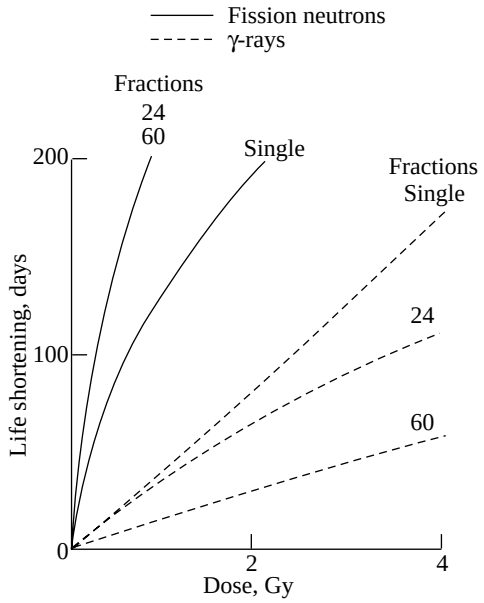

Figure 10. Dose protraction effects in mice with repair for low LET (γ-ray) and enhancement at high LET for fission neutron (ref. 15).

The uncertainties in radiation risk levels have been estimated in the Radiation Health Program (ref. 5) and are presented in figure 1. In the approximation used herein, it is assumed that the risk is related to the total value of dose equivalent and that the dose response curve is of similar shape for each radiation component. At low dose and dose rate, the response is linear. The excess risk is then

$$R = kH = k(H_x + H_z) \tag{9}$$

where H is dose equivalent (in Sv), H_x is the component of dose equivalent from low-LET radiation, and H_z is the dose equivalent that results from the HZE component of the radiation. We make the further approximation that the uncertainties in k and H_x are negligible compared with the uncertainty in H_z and obtain

$$\Delta R = k\frac{\Delta H_z}{H_z}H_z \equiv kUH_z \tag{10}$$

so that the net effect of the uncertainty in R is to increase the relative risk, which becomes

$$R + \Delta R = kH + kUH_z = kH_u \tag{11}$$

This equation defines an effective dose equivalent H_u that corresponds to the increased risk from uncertainties. If a limit L is defined on the basis of excess risk R, it is required that

$$R + \Delta R \leq L \tag{12}$$

A safety factor S can be defined with reference to equation (11). Let S be an upper bound on the estimated value of the uncertainty in the HZE dose equivalent and $S = nU$, where $n = 1, 2, \ldots$ corresponds to the number of standard deviations required to establish an acceptable safety margin. Then equation (11) becomes

$$R + \Delta R = kH + kSH_z = kH_s \tag{13}$$

where the effective dose equivalent, including the safety factor, is given by $H_s = H + SH_z$; alternatively, the HZE component in equation (9) can be increased according to $H_z' = H_z + SH_z = (1+S)H_z$. This equation suggests the possibility of using the ratio between experimental values of RBE (as appropriate for GCR exposure) and $\overline{Q}$ as an approximation for $1 + S$; for example, the measured RBE for life shortening in mice has been reported as large as 80 for fission neutrons (ref. 15), while the estimated value of $\overline{Q}$ is on the order of 20. Thus, an estimate for the value of S would be 3, which corresponds to an effective dose equivalent 300 percent greater for HZE exposure than would be obtained from currently accepted dosimetric analyses. Such a value (300 percent) might be considered reasonable from a radiobiological point of view and may not be too restrictive on mission design and operations. Normally high RBE values are associated with stochastic effects, and it is clear from figure 7 that cell killing has large RBE's for HZE exposure. Since cell killing is the assumed cause of early response, high RBE's are indicated.

Effects of Uncertainty on Shield Design

An astronaut on a lunar or martian mission is exposed to low-level GCR and is subject to the possibility of a large SEP event. We consider only the exposure of the blood forming organs (BFO), which is closely related to whole-body exposure and overall life shortening due to neoplastic disease. The solar minimum environment (maximum exposure) as prescribed by the cosmic ray effects on microelectronics

(CREME) model of the Naval Research Laboratory (ref. 16) is assumed, since the mission time is not yet specified. The CREME model underestimates the actual environment by at least 25 percent. The observed SEP's are variable in spectral characteristics and intensities, so that for design considerations, we assume an SEP model that consists of the spectrum envelope that bounds the (estimated) observed fluence at any observed energy. This spectrum is similar to the Viking mission design criteria[2] except that the envelope is now given by the February 1956, November 1960, and August 1972 events, as shown in figure 11. The differential fluence spectral envelope $\varphi(E)$ is determined by expressions derived from the individual flare spectral characteristics (ref. 17) and is given analytically as

$$\varphi(E) = \max(f_1, f_2, f_3) \tag{14}$$

where

$$f_1 \equiv 6.0 \times 10^7 \exp[-(E-10)/25] + 9.4E + 05 \exp[-(E-100)/320]$$

$$f_2 \equiv 6.3 \times 10^8 \exp[-(E-10)/12] + 4.9E + 06 \exp[-(E-100)/80]$$

$$f_3 \equiv 3.0 \times 10^8 \exp[-(E-30)/26.5]$$

In the above equation, E is energy in MeV and φ is in protons/cm^2-MeV. The f_1, f_2, and f_3 symbols represent fluences for the 1956, 1960, and 1972 flares, respectively. Of these three events, the 1972 event spectrum is best known through deep space measurements, the 1960 event spectrum is less well-known while the 1956 event spectrum is only crudely known to about a factor of two.

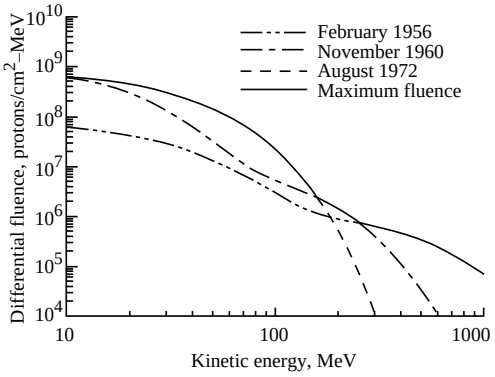

Figure 11. An estimate for the maximum fluence spectrum for an SEP event.

[2]NASA Viking Project Office Report: *Viking Project 75*; April 1972, (M75-125-2).

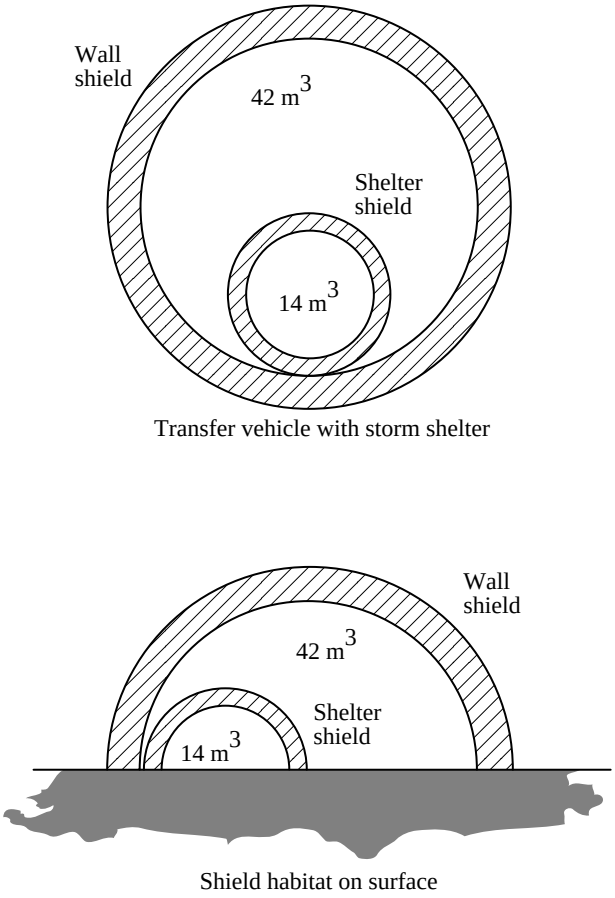

Figure 12. Models used for transfer vehicle and habitat configurations.

The total BFO dose equivalent as a function of shield thickness for a water-equivalent shield has been calculated using the nucleon transport code BRYNTRN (ref. 18) for the flare spectrum, and the nucleon/heavy-ion transport code HZETRN (ref. 19) for the GCR contribution. The body geometry is the computerized anatomical man model (CAM) from reference 20. The assumed quality factor is specified by ICRP-26 (ref. 21). For simplicity, shield configurations are taken as spherical shells of constant thickness, and dose evaluations are made at the center of the sphere, as shown in figure 12. For the living space, a minimum interior volume corresponding to reasonable astronaut performance (10.5 m^3/person, ref. 22) for a four-member crew is assumed. The storm shelter is assumed to be one-third as large as the living space. The variation of dose equivalent with shell thickness is evaluated for two configurations: a complete spherical shell representing a lunar transfer vehicle (LTV) in cis-lunar space or a martian transfer vehicle (MTV), and a hemispherical shell representing a habitat on the lunar or martian

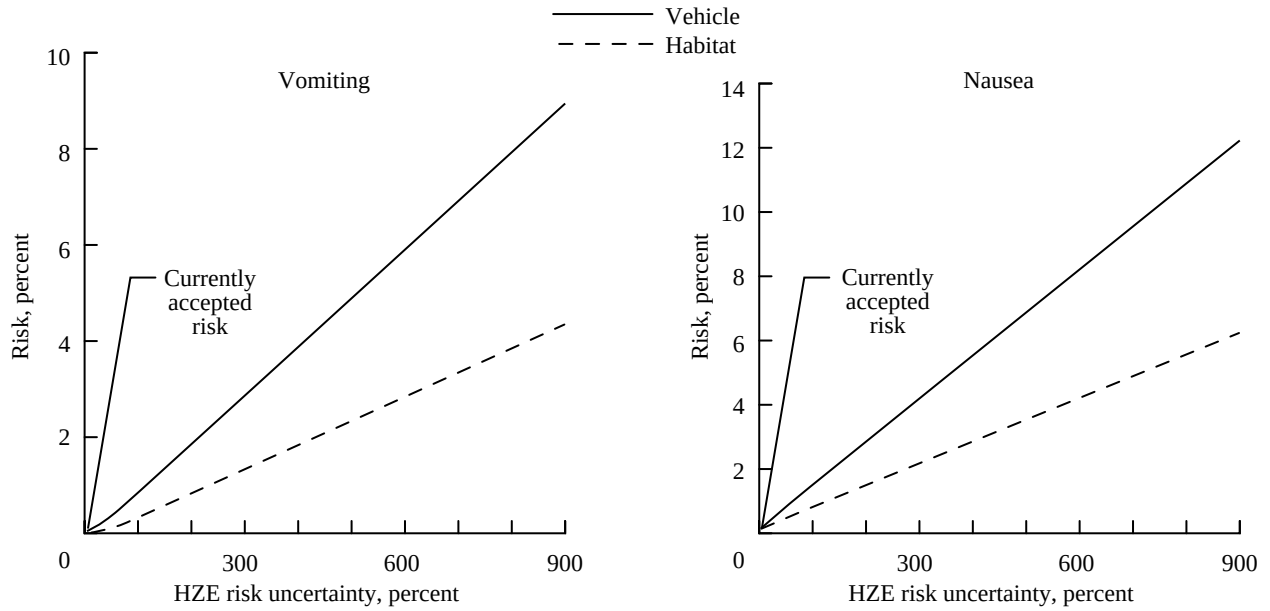

Figure 13. Risk of early responses occurring to astronauts exposed to SEP in vehicles or habitats for a 60-day lunar mission nominal design.

surface. We estimate the risk by accumulating the 30-day GCR exposure within the living quarters with negligible repair and no dose-rate enhancements as the background levels at the start of an SEP event. A nominal shelter design is determined by limiting the background exposure plus solar-event exposure to less than 0.25 Sv for any 30-day period (ref. 1). The nominal wall thickness is determined by limiting the excess fatal cancer risk to 3 percent. The nominal wall thickness must be at least that of the pressure vessel and meteoroid bumper (assumed to be 2 g/cm^2 of aluminum). These assumptions are perhaps pessimistic but consistent with our current stated knowledge of uncertainty.

Table III. Nominal Shield for Lunar and Martian Missions

	Shielding, g/cm^2 Al, for—			
	Lunar missions		Martian missions	
Shield location	60 days	6 months	18 months	29 months
Vehicle wall	2	2	5.9	3.8
Vehicle shelter	46	46	36.4	41.1
Habitat wall	2	2	17	17
Habitat shelter	7	7	0	0

A 60-Day Lunar Mission

The dose equivalents have also been computed for a mission duration of 60 days, 45 days on the lunar surface and 5 days transit time each way, with 5 days total spent in low Earth orbit. The transmitted doses of the LTV and habitat shields differ by a factor of two as a result of shielding of the habitat by the Moon. The BFO dose equivalents have been evaluated according to the human body geometry specified by the computerized anatomical man (ref. 20). We assume that the BFO exposure is indicative of the whole-body exposure. The nominal shield amounts are given in table III.

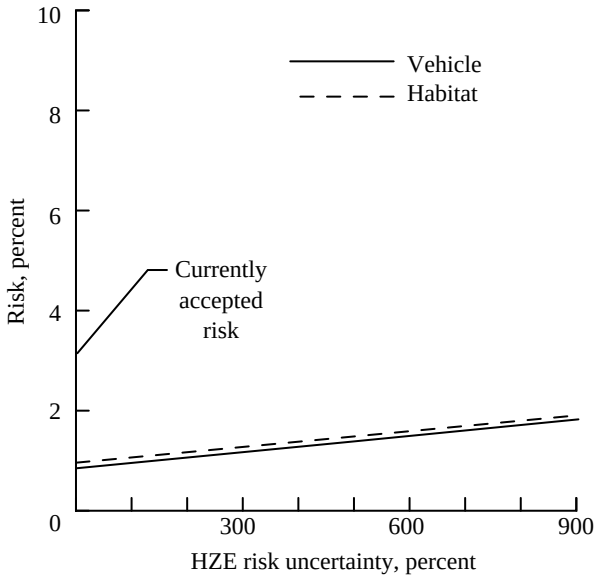

Figure 14. Excess fatal cancer risk for astronauts exposed to SEP in vehicles and habitats for a 60-day lunar mission nominal design.

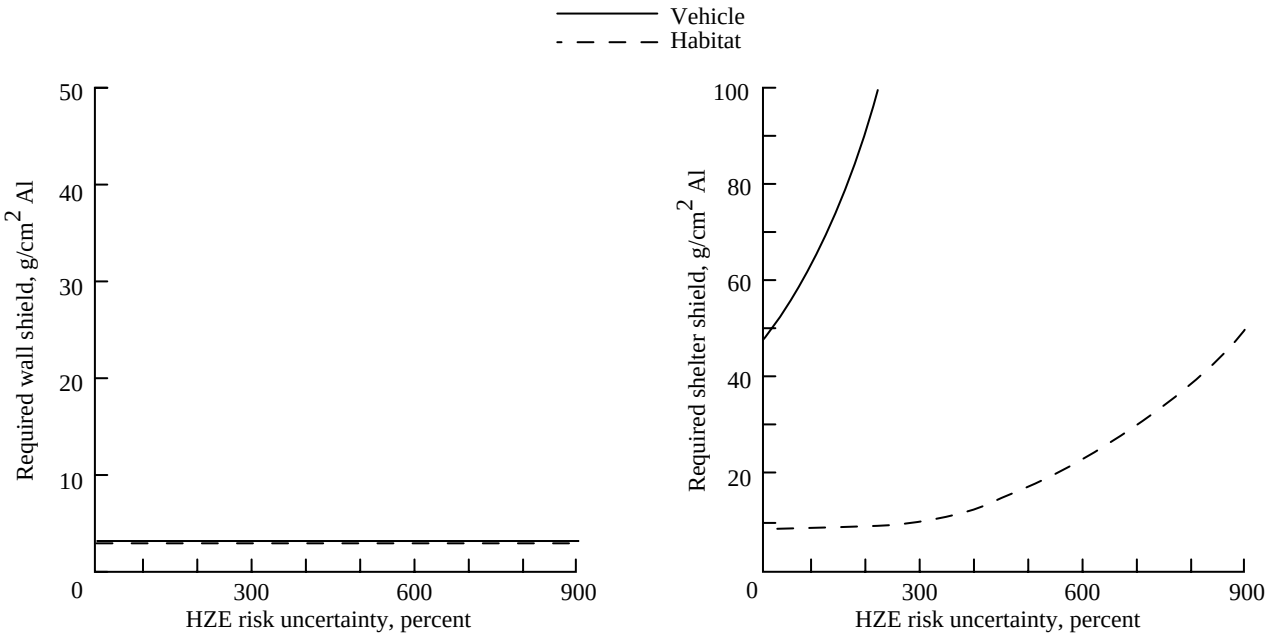

Figure 15. Required shield for walls and shelters to protect astronauts from SEP for 60-day lunar mission.

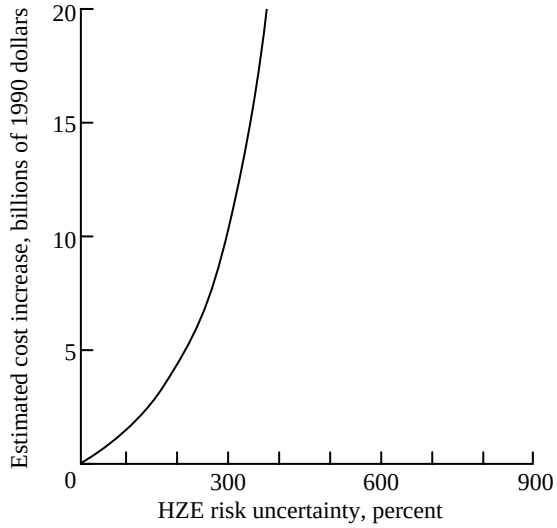

Figure 16. Excess mission cost from added shielding for vehicle and habitat to ensure astronaut safety for 60-day lunar mission.

The risk of early response for the nominal design is calculated by using equation (11) and the 1σ early response functions in figure 4. In the estimates, we assumed that the SEP event occurred while in transit (vehicle) or while on station (habitat). The risks of nausea and vomiting are shown in figure 13. The nominal design for no uncertainty shows zero risk as expected, but finite risks are obtained at the higher levels of uncertainty (risks may be affected by other stress factors, which tend to elicit these responses during the mission). The excess fatal cancer risk is shown in figure 14. The required shield amount for the walls and shelters is shown in figure 15, and the cost above the nominal design is shown in figure 16. The excess cost was estimated on the basis of the cost of the Apollo mission to deliver the lander and associated equipment to the lunar surface. We use the \$93 billion (1990) estimated by the Augustine Commission (ref. 23) for the Apollo program to deliver 800 000 lb (ref. 24) to the lunar surface. This amount corresponds to the \$116 250/lb or \$255 million/metric ton. It is clear from figure 16 that the excess cost at the 300-percent uncertainty level is about \$7 billion dollars over the nominal mission design.

A 6-Month Lunar Mission

The nominal shield design for a 6-month mission is shown in table III; this design is the same as for the 60-day mission, since the risks of early effects as a function of uncertainty are determined by the 30-day exposures and are the same as for the 60-day mission (fig. 17). The excess fatal cancer risk (fig. 18) is within 3 percent for uncertainties below 700 percent. An increased wall thickness is required for the habitat above the 700-percent level. The required thicknesses for the walls and shelters are shown in figure 19, and the excess mission cost is shown in figure 20. The effects of the increased habitat wall thickness

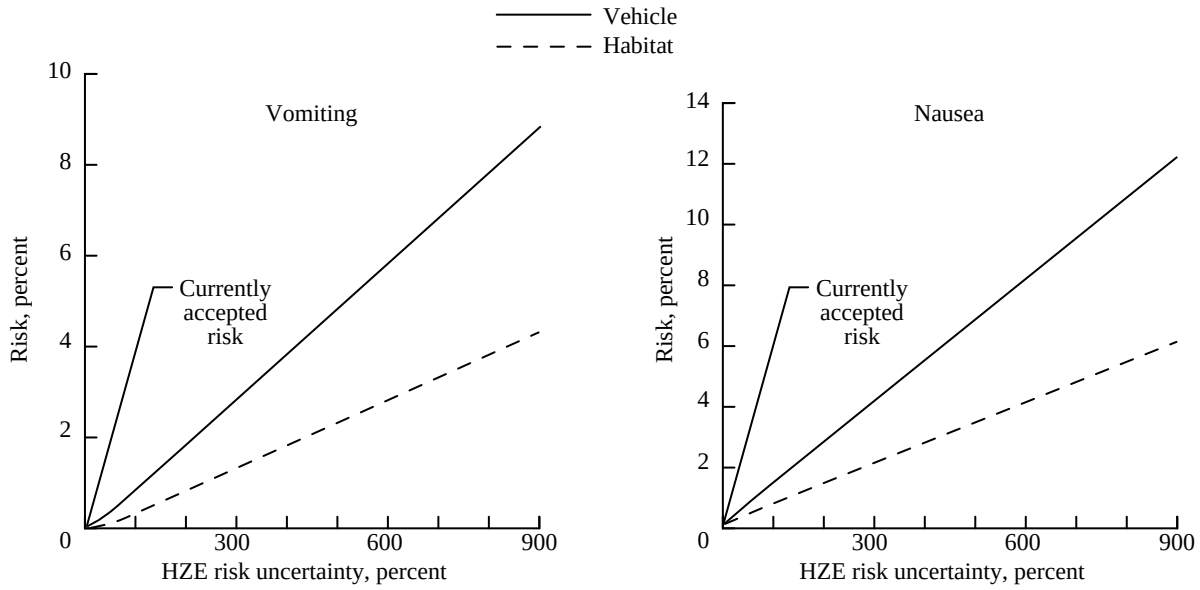

Figure 17. Risk of early response occurring to astronauts exposed to SEP in vehicles or habitats for 6-month lunar mission nominal design.

required to limit the fatal cancer risk are seen above 700 percent. (The excess shield cost is estimated for the 6-month mission and is similar to the excess cost of the 60-day mission.)

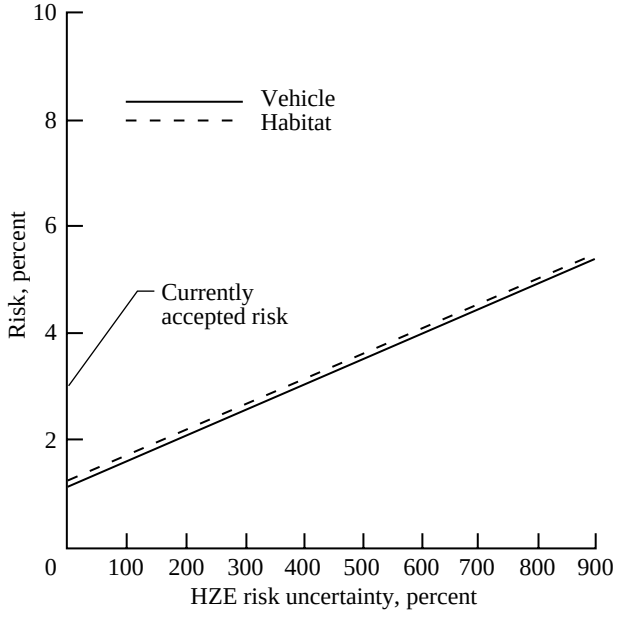

Figure 18. Excess fatal cancer risk for astronauts exposed to SEP in vehicles or habitats for 6-month lunar mission nominal design.

An 18-Month Martian Mission

The nominal shield design for the 18-month mission to Mars is shown in table III. The wall thickness of the vehicle is designed to limit the excess fatal cancer risk for the mission to 3 percent. The habitat wall thickness is the minimum required for a pressure vessel (2 g/cm^2) plus the atmosphere overhead (15 g/cm^2); the wall is unaffected by the fatal cancer risk, since only 30 days are assumed for the on-station exposure. Moreover, because of the natural protection by the atmosphere, the need for separate shelter in the habitat for protection from solar flares is precluded. The increased risk of early response due to uncertainties is different from the risk for the lunar missions, as shown in figure 21. This difference is a result of the increased shielding of the martian atmosphere and of the living quarters in the nominal mission design. The excess fatal cancer risk could be unacceptable, approaching 15 percent at the 900-percent uncertainty level (fig. 22). The required shelter shield amount is controlled mainly by the required increase in wall thickness as a function of uncertainty (fig. 23). Hence, the required shelter shield decreases as the vehicle wall increases. The excess mission costs shown in figure 24 are calculated under the assumption that a mission to Mars is four times as expensive as the lunar mission (ref. 23).

A 29-Month Martian Mission

This mission has substantially different circumstances than the previously described short-stay martian mission; transit times have been reduced and stay time has increased greatly. Both outbound and inbound voyages will be 5 months, with time spent on the planet surface set at 19 months (refs. 25 and 26). Table III gives the nominal shield design

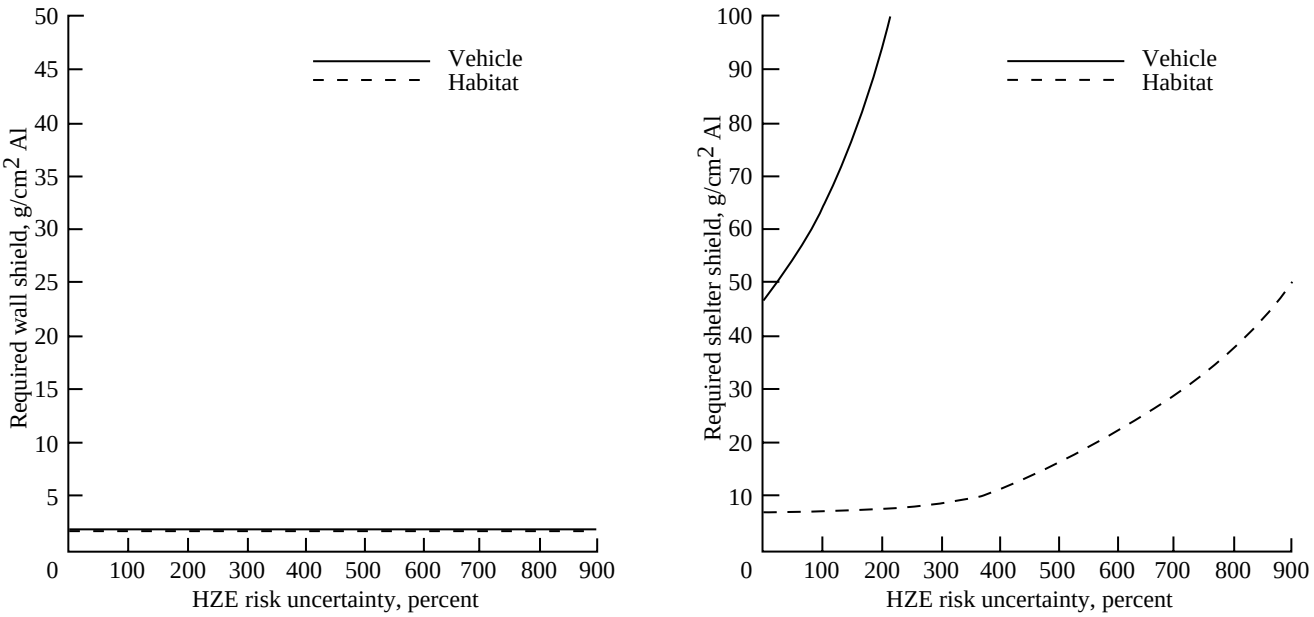

Figure 19. Required shield for walls and shelters to protect astronauts from SEP for 6-month lunar mission.

thicknesses, and the requirements are again to limit excess fatal cancer risk to 3 percent. As for the 18-month mission to Mars, the habitat protection at the planet is prescribed as the nominal pressure vessel thickness (2 g/cm^2) plus the overhead atmosphere amount (15 g/cm^2). The increase of fatal cancer risk with HZE uncertainty (fig. 25) is greater because of the longer total mission duration, but only slightly so; excess risk is again on the order of 15 percent at 900-percent uncertainty. The early response effects (nausea, vomiting) have been assessed for this mission; as expected, they are almost identical with those for the 18-month mission (fig. 21).

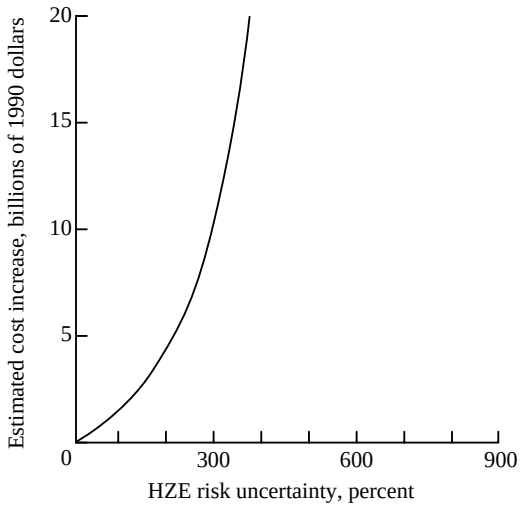

Figure 20. Excess mission cost from added shielding for vehicle and habitat to ensure astronaut safety for 6-month lunar mission.

Figure 26 shows the required shield amounts for the 29-month mission; where as for the 18-month mission, the required vehicle shield for shelter from an SEP event in transit decreases as the vehicle wall thickness grows. Because of the shorter travel times, the wall thickness growth with HZE uncertainty is less noticeable than for the 18-month mission. As a consequence, the corresponding rise of estimated cost is also less (fig. 27).

Discussion of Results

The present study relates the current estimates of biological uncertainty (ref. 5) to the practical problems of engineering design and mission cost. An earlier attempt to present the effects of biological uncertainties based on the use of dose limits as action levels (ref. 27) did not give a clear presentation of the potential for added risk for the uncertainty level assumed. The present report in which potential risk increase is presented explicitly provides operational guidance with respect to redesign considerations. For example, a 15-percent risk of nausea within a 2-day period following a solar flare is not necessarily unacceptable and may be preferred to a substantial increase in mission cost. Conversely, a 15-percent excess risk of fatal cancer may not be justifiable and will require costly redesign. The advantage of risk-based models is aptly demonstrated.

Still in developing a risk-based approach to space radiation protection, there are many issues to be

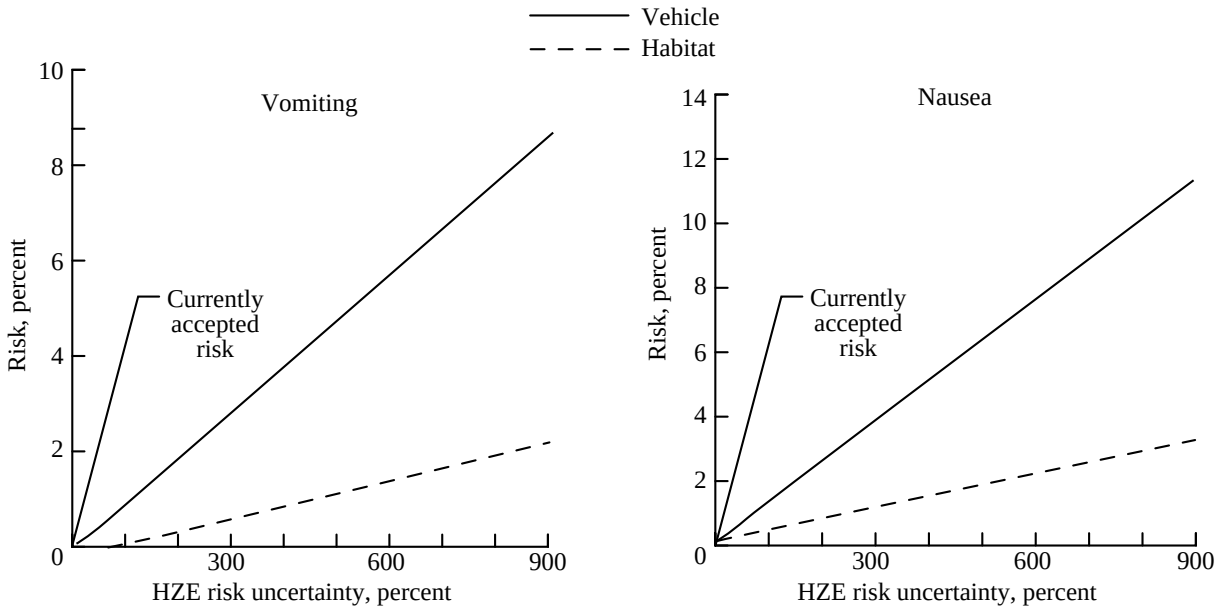

Figure 21. Risk of early responses occurring to astronauts exposed to SEP in vehicles or habitats for 18-month mission to Mars nominal design.

resolved. The primary issue is that for human radiation response, data are known mainly for the high dose-rate γ-ray exposures from nuclear weapons used in World War II. The practical use of these data for fractionated or low dose rate exposures over many years cannot be solved without some assessment of radiation injury repair rates and repair efficiencies, which vary greatly among the various cell populations within the human body.

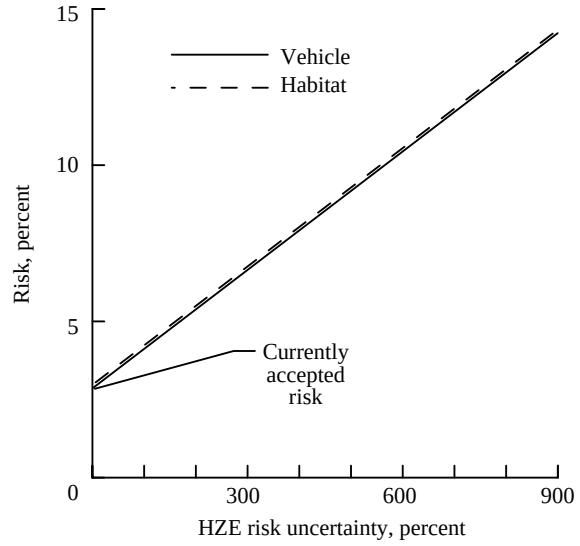

Figure 22. Excess fatal cancer risk for astronauts exposed to SEP in vehicles and habitats for 18-month mission to Mars nominal design.

A second but not unrelated issue is the extrapolation of the γ-ray data to other radiation types. The historical approach examined the RBE of a set of relevant biological end points in animal exposures for radiations of different quality (denoted by the value of LET) and defined a quality factor Q(LET) as a conservative upper limit of the RBE for the relevant end points. As the RBE values depended on levels of exposure and dose rates, the maximum RBE values were found to be exceedingly large (table II). Again, such large RBE values are related to repair rates and repair efficiencies (ref. 28) and must be reflected in risk assessment methods. Some of the repair aspects of fluence-based risk coefficients (ref. 29) are discussed elsewhere (ref. 30) and may provide one approach to this issue. A second approach would be to couple cell response models with tissue system models for evaluation of risk (ref. 28). The approach in this paper was to examine the impact on future NASA missions of using current estimated biological uncertainty. It is clear that such uncertainties may result in a large additional dollar cost to missions to the Moon and Mars. Furthermore, the reduction of these uncertainties and development of improved risk models will have an important impact on mission operations and would substantially reduce mission cost. The cost of this biological research and model development is small when compared with the projected increase in mission cost because of the uncertainties discussed herein.

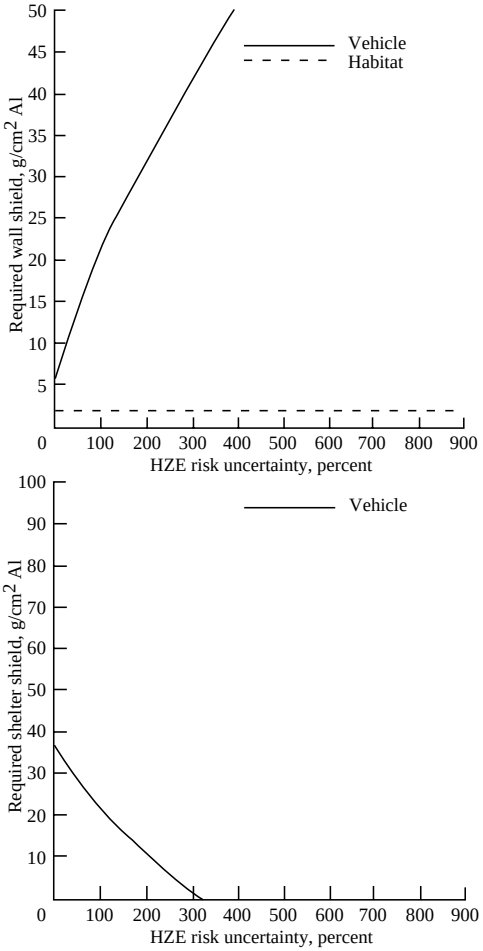

Figure 23. Required shield for walls and shelters to protect astronauts from SEP for 18-month mission to Mars.

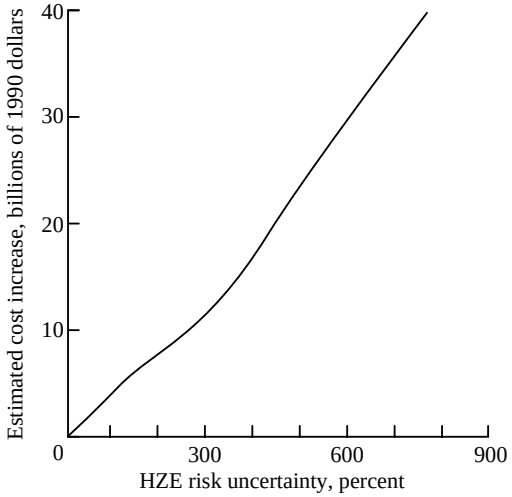

Figure 24. Excess mission cost from added shielding for vehicle and habitat to ensure astronaut safety for 18-month Mars mission.

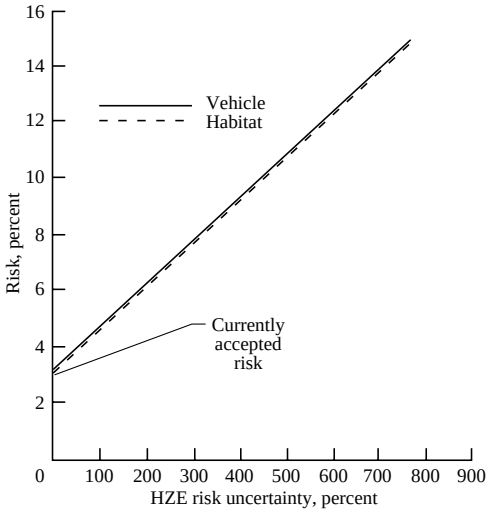

Figure 25. Excess fatal cancer risk for astronauts exposed to SEP in vehicles or habitats for 29-month Mars mission nominal design.

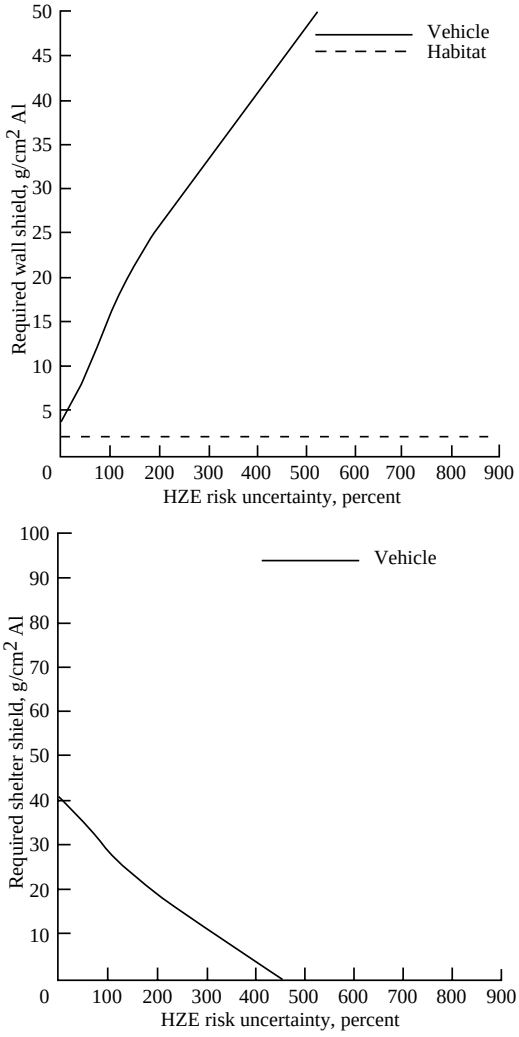

Figure 26. Required shield for walls and shelters to protect astronauts from SEP for 29-month mission to Mars.

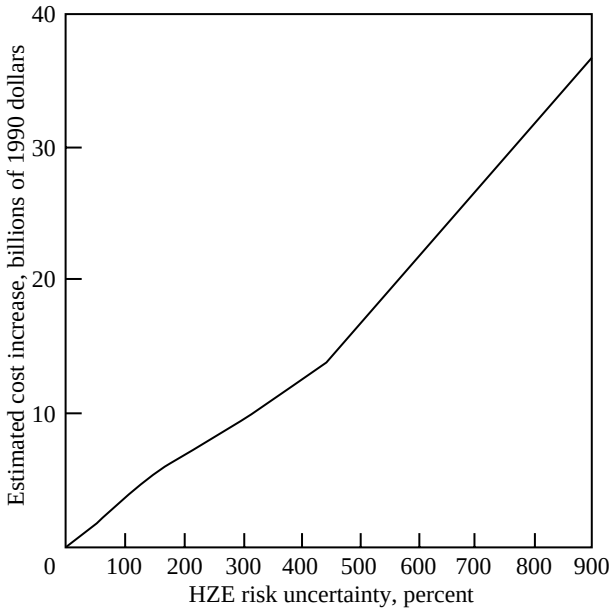

Figure 27. Excess mission cost from added shielding for vehicle and habitat to ensure astronaut safety for 29-month Mars mission.

Concluding Remarks

The effect of risk uncertainties due to heavy-ion galactic cosmic ray (GCR) exposure for relatively short-duration lunar missions has been analyzed. The results indicate that shield design and mission cost are significantly affected by these uncertainties. The analysis does not explicitly include the effect of uncertainties in the properties of the shielding materials (including uncertainties in radiation transport), the dependence of risk coefficients on linear energy transfer (LET), the quadratic terms in the dose response function, the dependence of risk on dose rate, and other effects that may need to be considered for special circumstances or longer duration missions. Shield requirements have been estimated for simple configurations in a severe (but not necessarily unreasonable) worst-case solar flare environment. Because of the importance of the high-energy spectrum of the February 1956 event, some effort should be made to improve our knowledge of this event. The results show that GCR risk uncertainties can dramatically impact many lunar mission parameters; therefore, such calculations need to be incorporated into engineering design considerations at an early stage. The methods were applied to a 60-day lunar mission and had a similar impact on mission design for the 6-month mission. Further analysis of 18-month and 29-month missions to Mars also reveals a large impact on the missions, resulting in tens of billions of dollars in excess mission cost to ensure safe designs. Finally, the calculation presented herein offers a new approach to understanding the cost-effectiveness of investment in radiation physics and radiobiological research.

NASA Langley Research Center
Hampton, VA 23681-0001
May 6, 1993

References

1. National Council on Radiation Protection and Measurements: *Guidance on Radiation Received in Space Activities.* NCRP Rep. No. 98, July 31, 1989.

2. Aghamohammadi, S. Z.; Goodhead, D. T.; and Savage, J. R.: Induction of Sister Chromatid Exchanges (SCE) in GO Lymphocytes by Plutonium-238 Alpha-Particles. *Int. J. Radiat. Biol. & Relat. Stud. Phys., Chem. & Med.,* vol. 53, no. 6, June 1988, pp. 909–915.

3. Kadhim, M. A.; Macdonald, D. A.; Goodhead, D. T.; Lorimore, S. A.; Marsden, S. J.; and Wright, E. G.: Transmission of Chromosomal Instability After Plutonium α-Particle Irradiation. *Nature,* vol. 355, no. 6362, Feb. 20, 1992, pp. 738–740.

4. Kraft, G.: Radiobiological Effects of Very Heavy Ions: Inactivation, Induction of Chromosome Aberrations and Strand Breaks. *Nucl. Sci. Appl.,* sect. A, vol. 3, no. 1, 1987, pp. 1–28.

5. Schimmerling, Walter: Radiobiological Problems in Space—An Overview. *Radiat. & Environ. Biophys.,* vol. 31, 1992, pp. 197–203.

6. Townsend, Lawrence W.; Nealy, John E.; Wilson, John W.; and Simonsen, Lisa C.: *Estimates of Galactic Cosmic Ray Shielding Requirements During Solar Minimum.* NASA TM-4167, 1990.

7. *1990 Recommendations of the International Commission on Radiological Protection.* ICRP Publ. 60, Pergamon Press Inc., c.1991.

8. Langham, Wright H., ed.: *Radiobiological Factors in Manned Space Flight.* National Academy of Sciences, National Research Council, 1967.

9. Committee on the Biological Effects of Ionizing Radiations: *Health Effects of Exposure to Low Levels of Ionizing Radiation.* BEIR V, National Academy Press, 1990.

10. Bond, V. P.; Varma, M. N.; and Sondhaus, C. A.: The RBE Concept, Its Inadequacies and a Suggested Replacement. *Mechanisms of Radiation Interaction With DNA: Potential Implications for Radiation Protection,* CONF-870163, U.S. Dep. of Energy, 1988, pp. 31–38.

11. *The Quality Factor in Radiation Protection.* ICRU Rep. 40, International Commission on Radiation Units and Measurements, Apr. 4, 1986.

12. Wilson, John W.; and Cucinotta, Francis A.: *Cellular Repair/Misrepair Track Model.* NASA TP-3124, 1991.

13. Todd, Paul: Unique Biological Aspects of Radiation Hazards—An Overview. *Adv. Space Res.,* vol. 3, no. 8, 1983, pp. 187–194.

14. Scott, B. R.: Methodologies for Predicting the Expected Combined Stochastic Radiobiological Effects of Different Ionizing Radiations and Some Applications. *Radiat. Res.,* vol. 98, no. 1, Apr. 1984, pp. 182–197.

15. Thomson, John F.; and Grahn, Douglas: Life Shortening in Mice Exposed to Fission Neutrons and γ Rays. VII. Effects of 60 Once-Weekly Exposures. *Radiat. Res.,* vol. 115, 1988, pp. 347–360.

16. Adams, J. H., Jr.; Silberberg, R.; and Tsao, C. H.: *Cosmic Ray Effects on Microelectronics. Part I—The Near-Earth Particle Environment.* NRL Memo. Rep. 4506-Pt. I, U.S. Navy, Aug. 1981. (Available from DTIC as AD A103 897.)

17. Wilson, John W.: Environmental Geophysics and SPS Shielding. *Workshop on the Radiation Environment of the Satellite Power System,* Walter Schimmerling and Stanley B. Curtis, eds., LBL-8581 (Contract W-7405-ENG-48), Univ. of California, Sept. 15, 1978, pp. 33–116.

18. Wilson, John W.; Townsend, Lawrence W.; Nealy, John E.; Chun, Sang Y.; Hong, B. S.; Buck, Warren W.; Lamkin, S. L.; Ganapol, Barry D.; Khan, Ferdous; and Cucinotta, Francis A.: *BRYNTRN: A Baryon Transport Model.* NASA TP-2887, 1989.

19. Wilson, John W.; Chun, Sang Y.; Badavi, Forooz F.; Townsend, Lawrence W.; and Lamkin, Stanley L.: *HZETRN: A Heavy Ion-Nucleon Transport Code for Space Radiations.* NASA TP-3146, 1991.

20. Billings, M. P.; and Yucker, W. R.: *The Computerized Anatomical Man (CAM) Model.* NASA CR-134043, 1973.

21. *Recommendations of the International Commission on Radiobiological Protection.* ICRP Publ. 26, Pergamon Press, Inc., c.1987.

22. *Man-Systems Integration Standards.* NASA-STD-3000, Volume I, NASA Johnson Space Center, Mar. 1987.

23. Augustine, Norman R.; and Wilkening, Laurel L.: *The Augustine Report (Report of the Advisory Committee on the Future of the U.S. Space Program),* U.S. House of Representatives Committee on Science, Space, and Technology, Jan. 1991.

24. Furniss, Tim: *Manned Spaceflight Log,* New ed. Jane's Publ. Inc., c.1986.

25. Striepe, Scott A.; Simonsen, Lisa C.; and Nealy, John E.: Radiation Exposure Predictions for Long-Duration-Stay Mars Missions. AIAA-92-4584, Aug. 1992.

26. Soldner, John K.; and Joosten, B. K.: Mars Trajectory Options for the Space Exploration Initiative. *Astrodynamics 1991—Proceedings of the AAS/AIAA Astrodynamics Conference,* Part 3, Univelt, Inc., 1992, pp. 1935–1948. (Available as AAS Paper 91-438.)

27. Wilson, John W.; Nealy, John E.; and Schimmerling, Walter: *Effects of Radiobiological Uncertainty on Shield Design for a 60-Day Lunar Mission.* NASA TM-4422, 1993.

28. Wilson, J. W.; Cucinotta, F. A.; and Shinn, J. L.: Cell Kinetics and Track Structure. Paper presented at NATO Advanced Study Institute Conference on Biological Effects and Physics of Solar and Galactic Cosmic Radiation (Armacao de Pêra, Algarve, Portugal), Oct. 12–23, 1991.

29. Curtis, S. B.; Townsend, L. W.; Wilson, J. W.; Powers-Risius, P.; Alpen, E. L.; and Fry, R. J. M.: Fluence-Related Risk Coefficients Using the Harderian Gland Data as an Example. *Adv. Space Res.,* vol. 12, no. 2–3, 1992, pp. (2)407–(2)416.

30. Wilson, John W.; Cucinotta, Francis A.; Shinn, Judy L.; and Townsend, Lawrence W.: *Target Fragmentation in Radiobiology.* NASA TM-4408, 1993.

REPORT DOCUMENTATION PAGE

Form Approved
OMB No. 0704-0188

1. AGENCY USE ONLY *(Leave blank)*	2. REPORT DATE	3. REPORT TYPE AND DATES COVERED
	August 1993	Technical Paper

4. TITLE AND SUBTITLE
Effects of Radiobiological Uncertainty on Vehicle and Habitat Shield Design for Missions to the Moon and Mars

5. FUNDING NUMBERS
WU 199-04-16-11

6. AUTHOR(S)
John W. Wilson, John E. Nealy, Walter Schimmerling, Francis A. Cucinotta, and James S. Wood

7. PERFORMING ORGANIZATION NAME(S) AND ADDRESS(ES)
NASA Langley Research Center
Hampton, VA 23681-0001

8. PERFORMING ORGANIZATION REPORT NUMBER
L-17188

9. SPONSORING/MONITORING AGENCY NAME(S) AND ADDRESS(ES)
National Aeronautics and Space Administration
Washington, DC 20546-0001

10. SPONSORING/MONITORING AGENCY REPORT NUMBER
NASA TP-3312

11. SUPPLEMENTARY NOTES
Wilson, Nealy, and Cucinotta: Langley Research Center, Hampton, VA; Schimmerling: Universities Space Research Association, Washington, DC; Wood: Flight Mechanics and Control, Inc., Hampton, VA.

12a. DISTRIBUTION/AVAILABILITY STATEMENT
Unclassified–Unlimited

Subject Category 93

12b. DISTRIBUTION CODE

13. ABSTRACT *(Maximum 200 words)*

Some consequences of uncertainties in radiobiological risk due to galactic cosmic ray (GCR) exposure are analyzed for their effect on engineering designs for the first lunar outpost and a mission to explore Mars. This report presents the plausible effect of biological uncertainties, the design changes necessary to reduce the uncertainties to acceptable levels for a safe mission, and an evaluation of the mission redesign cost. Estimates of the amount of shield mass required to compensate for radiobiological uncertainty are given for a simplified vehicle and habitat. The additional amount of shield mass required to provide a safety factor for uncertainty compensation is calculated from the expected response to GCR exposure. The amount of shield mass greatly increases in the estimated range of biological uncertainty, thus escalating the estimated cost of the mission. The estimates are used as a quantitative example for the cost-effectiveness of research in radiation biophysics and radiation physics.

14. SUBJECT TERMS	15. NUMBER OF PAGES
Radiation; Space; Risk	18
	16. PRICE CODE: A03

17. SECURITY CLASSIFICATION OF REPORT	18. SECURITY CLASSIFICATION OF THIS PAGE	19. SECURITY CLASSIFICATION OF ABSTRACT	20. LIMITATION OF ABSTRACT
Unclassified	Unclassified		